Journal of the Indian Institute of Science
A Multidisciplinary Reviews Journal
ISSN: 0970-4140 Coden-JIISAD

REVIEWS

Region of Interest Compressed Sensing MRI

*Amaresha Shridhar Konar[a], Jain A. Divya[a], Shamshia Tabassum[a], Rajagopalan Sundaresan[c], Julianna Czum[b], Barjor Gimi[b], Ramesh Babu D.R.[a], Ramesh Venkatesan[c] and Sairam Geethanath[a]**

Abstract | Compressed Sensing (CS) based Magnetic Resonance Imaging (MRI) reconstruction relies on data sparsity. Region of Interest Compressed Sensing (ROICS) is based on the hypothesis that superior CS performance can be obtained by limiting the sparsity objective and data consistency in CS to a Region of Interest (ROI). This relaxation is justified in most applications where the anatomy of interest such as the heart, has surrounding structures, typically not used for further analyses. ROICS has been proposed as an extension of CS that is ROI weighted CS. Current work demonstrates the implementation of ROICS for the first time on MR cardiac and brain data. Reconstructed images and performance evaluation metrics show that ROICS technique performs better than conventional CS technique. CS and Parallel Imaging (PI) are widely used to reduce MRI scan time and their combination yields better performance than used individually. The proposed method also implements the combination of ROICS and SENSitivity Encoding (SENSE), which applies weighted CS to a particular ROI, and the resulting output is then reconstructed using SENSE for arbitrary k-space. Proposed ROICS-PI performs better as compared to PI and CS + PI.

1 Introduction

Magnetic Resonance Imaging (MRI) is a well-established whole body imaging modality, which provides soft tissue contrast at high resolution. It has therefore been extensively used in the diagnosis and/or prognosis of various pathological conditions ranging from cancer to psychiatric diseases. However, the acquisition time required for MRI is longer as compared to other whole-body imaging modalities such as Computed Tomography (CT) and Positron Emission Tomography (PET). This limits the spatial and temporal resolutions required for imaging of critical physiological processes that have to be imaged rapidly. Prolonged acquisition time results in patient discomfort and motion artefacts. Two examples of such cases are imaging of the heart and contrast enhanced MRI. A compromise on spatial resolution adversely affects morphology, while poor temporal resolution impacts clinical analyses of functions of the organ system. The current work aims to accelerate MRI scan time based on the framework of CS. CS[1,2] and PI[3] are two well-known approaches in MRI to reduce acquisition time. CS aims to reconstruct signals and images from significantly fewer measurements than were traditionally thought necessary. CS relies significantly on transform data to enable reconstruction of images with high fidelity from highly undersampled k-space data. This implies that increased sparsity provides better CS reconstruction at increased accelerations.[4] The application of CS on diverse MR methods has been successfully demonstrated such as in dynamic MRI to accelerate the image reconstruction through kt FOCUS.[5] In this work, a novel technique called 'Region of Interest Compressed Sensing (ROICS)' is proposed.[6] ROICS is based on the hypothesis that superior CS performance can be obtained by limiting the CS

[a]*Medical Imaging Research Center (MIRC), Dayananda Sagar Institutions, Bangalore, India.*

[b]*Department of Radiology, Giesel School of Medicine, Dartmouth, USA.*

[c]*Wipro-GE Healthcare, Bangalore, India.*

**sairam.geethanath@dayanandasagar.edu*

framework to a ROI. This relaxation is justified in most applications where the anatomy of interest such as the heart has surrounding structures, and the background is typically not important for further analyses. The images resulting from an MR acquisition are typically sparse in the wavelet representation and/or total variation norm, and hence lend themselves well to ROICS. The inclusion of such a region weighting mask for the sparsity objective and data consistency enhances sparsity in the reconstruction, which implies reduction in the number of data samples required for reconstruction. This would hence result in acceptable reconstructions even at higher accelerations. Combination of CS and PI results in increased performance than using either of them individually, and this combination has been demonstrated on MRI methods.[7–15] In this work, ROICS is combined with PI for an arbitrary k-space trajectory to provide superior performance as compared to CS-PI. PI is a robust method for accelerating the acquisition of MRI data, thereby reducing the scan time. PI achieves acceleration through undersampling of k-space while learning from the sensitivities of multiple receiver coils. These undersampled data can be acquired more quickly, but the undersampling leads to aliased images due to the violation of Nyquist criteria and has a direct impact on the Signal to Noise Ratio (SNR) of the Reconstructed images. One of several PI algorithms can be used to reconstruct artifact-free images from either the aliased images (SENSE-type reconstruction) or from the undersampled data (GRAPPA-type reconstruction). The advantages of PI include faster image acquisition, which can be used for instance, to shorten breath-hold times resulting in fewer motion-corrupted examinations. However, PI is also SNR dependent, and hence is limited in cases of low SNR acquisitions because the signal is divided amongst as many numbers of images as the receiver array, reducing the overall signal. ROICS reconstruction performed on each channel will exploit data sparsity that would result in increased SNR through Removal of Incoherent noise in the ROI, and hence provide for a better input for the subsequent PI based reconstruction.[16]

2 Theory

ROICS: The formulation for ROICS can be derived from the unconstrained convex optimization functional for conventional CS represented by Eq. [1]

$$\min_m (\| F_u(m) - y \|_2 + \lambda \| \psi(m) \|_1) \qquad (1)$$

where, m is the current estimate of the image to be obtained, F_u is the undersampled orthonormal Fourier operator: $F(.)*$ Undersampling mask, y is the undersampled k-space measured by the acquisition process, λ is the regularization factor, determined by methods like Tikhonov regularization or L-curve optimization,[17] Ψ is the sparsifying transform operator and $\|.\|_k$ is the k-norm operator. The unconstrained CS problem in Eq. [1] can be solved with the data consistency evaluation performed in the image domain. Eq. [1] can be re-written as:

$$\min_m (\| F^{-1}(F_u(m) - y) \|_2 + \lambda \| \psi(m) \|_1) \qquad (2)$$

where, F^{-1} is the inverse Fourier transform. The data consistency term is evaluated in the spatial domain as opposed to the k-space and is equivalent to Eq. [1] (Parseval's theorem as applied for the orthonormal Fourier transform). ROICS can be derived from Eq. [2] by weighting the spatial data consistency term over a ROI, described by a diagonal matrix W of size (Ns*Ns), where Ns is the product of the number of rows and columns of the image. The use of spatial weighting has also been used elsewhere.[18] This results in Eq. [3],

$$\min_m (\| F^{-1}(F_u(m) - y) * W \|_2 + \lambda \| \psi(m * W) \|_1) \qquad (3)$$

The ROI relaxed functional now takes the form of Eq. [3], where W is the Ns*Ns diagonal matrix containing a spatial weighting that one can use to specify and evaluate a ROI, of the dimensions of the image. The inclusion of such a ROI mask enhances sparsity in the reconstruction, which implies reduction in the number of data samples required for reconstruction. This is achieved by relaxing the constraint on the data consistency term, and hence would allow for a sparser solution, as the optimization problem is more tolerant towards error from the data consistency term. This would hence result in better reconstructions at higher accelerations compared to conventional CS reconstructions with identical regularization factors and sparsity transforms. CS and ROICS reconstruction algorithms for retrospective reconstruction are detailed in Algorithm 1.

ROICS-PI: The ROICS formulation could be extended to integrate PI. Data acquired using multi-channel receiver coils simultaneously could be ROICS reconstructed per channel followed by PI reconstruction using methods such as SENSE[19] or GRAPPA[20] to yield the final image. We can rewrite Eq. [3] for each channel '*c*' with k-space acquired with an arbitrary trajectory to perform ROICS-PI. ROICS precedes PI as CS based reconstructions like ROICS are inherently designed for denoising,

Table 1: ROICS and ROICS-PI reconstruction algorithms (Retrospective).

Algorithm 1 Pseudo code of CS and ROICS reconstruction (retrospective)

```
Require: Raw MRIk-space data (without applying CS\PI)
Read full k-space data
Select the reference image to draw ROI
Choose the undersampling factor (acceleration factor)
Choose the reconstruction technique (CS or ROICS)
if reconstruction technique is CS
    for all frames CS reconstruction using equation (1)
        end for
end for if
else (Reconstruction technique is ROICS)
for all frames ROICS reconstruction using equation (3)
    end for
end for else
```

Algorithm 2 Pseudo code of CS-PI and ROICS-PI reconstruction (retrospective)

```
Read full k-space data in matlab
Select the reference image to draw ROI to select
common ROI for all channels
Chose the reconstruction technique (CS or ROICS)
if reconstruction technique is CS
    for all the channel data apply CS
        reconstruction using equation (1)
    end for
end for if
else (Reconstruction technique is ROICS)
    for all the channel data apply ROICS
        reconstruction using equation (4)
  end for
end for else
CS-PI and ROICS-PI reconstruction using previous
CS and ROICS reconstructed data respectively
using PI technique such as SENSE or GRAPPA using
equation (5)
```

while PI works well once the SNR of the signal has improved due to the ROICS reconstruction

$$\min_m (\| F_1^{-1}(F_{1u}(m_c) - y_c) * W \|_2 + \lambda \| \psi(m_c * W) \|_1) \tag{4}$$

where, F_{1u} is Non Uniform Fast Fourier Transform (NUFFT)[21] for arbitrary k-space trajectory applied on image estimate m_c and y_c is the k-space of the c^{th} channel. These channel images could be then reconstructed using Eq. [26] in,[22] reproduced here:

$$(IE^H DEI)b = a \tag{5}$$

where, a is the intermediate image, b is an approximation solution, I is intensity correction, E is the NUFFT of the coil sensitivity weighted image resulting in k-space, E^H is complex conjugate transpose of E and D is the density compensation factor. CS-PI and ROICS-PI reconstruction algorithms are detailed in Algorithm 2.

The advantage of using ROICS method is shown in Figure 1. It can observed that by limiting

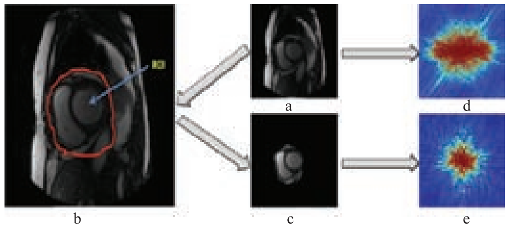

Figure 1: Selecting the ROI on cardiac frame and k-space comparison (a) Selected cardiac frame, (b) Selecting the ROI in the cardiac frame, (c) ROI selected, (d) k-space of the selected cardiac frame and, (e) k-space of the ROI selected at same window level.

the support in the image space (Figure 1(c)) that the extent of significant k-space values (indicated in terms of intensity in red and blue) has been also limited as seen in Figure 1(e). In other words, samples required to reconstruct the image from k-space are reduced. It is evident from the Figure 1 that the extent of k-space reduces with limiting the support of ROI.

3 Methods

ROICS was applied on cardiac and brain MRI. In all cases of reconstruction, the Nonlinear conjugate gradient (NCG)[23] method was used to solve the unconstrained optimization problem in Eqs. [1], [3] and [4].

ROICS on cardiac data: ROICS technique was applied to 10 cardiac frames selected from 10 different datasets of similar anatomy. MRI was performed on 10 human volunteers as part of an Institutional Review Board (IRB) approved MRI study. The acquisition consisted of a 2D multi-slab cardiac datasets acquired on 1.5T scanner with TR/TE = 5.09/1.42 ms, matrix size = 256 × 256 with slice thickness of 8 mm using contrast agent Magnevist. The selected frames were then reconstructed retrospectively by undersampling k-space at factors of 0.5, 0.33, 0.25, 0.2, 0.125, 0.1 equivalent to 2×, 3×, 4×, 5×, 8×, 10× respectively, using conventional CS, Eq. [1] and ROICS, Eq. [3]. ROI was selected in image by considering only the heart region, since surrounding structure was not required for further analyses as shown in Figure 1(b). ROI mask with binary values, ones (1's) within the ROI and zeros (0's) outside the ROI. This mask was used to implement the ROICS. The error of reconstruction was quantified by the Normalized Root Mean Square Error (NRMSE) metric using the formula

$$RMSE = \sqrt{\frac{\sum_{i=1}^{n} (x_p - x_r)^2}{N}}, \tag{6}$$

where x_p, x_r are the CS/ROICS reconstructed and full k-space reconstructed image respectively, and N is number of elements in x_p or x_r.

NRMSE was obtained by normalizing the RMSE to the range of the observed data. Average NRMSE values for 10 frames at different accelerations were calculated for both conventional CS and ROICS for only ROI chosen area in both cases.

ROICS-PI: The technique was applied on 6 human brain datasets acquired using a 1.5T scanner, as part of an ERB approved protocol, in coronal orientation and a spin echo sequence using 6 receiver coils (TR/TE = 410/8.7 ms, matrix size = 512 × 256) with no CS or PI turned on during acquisition. ROICS was applied to each channel data by selecting a common ROI across all channels (marked in red in Figure 3(a)) after retrospectively undersampling k-space data with a variable density spiral trajectory consisting of 64, 48, 32 and 16 interleaves. Images were reconstructed at these values of interleaves corresponding to acceleration factors of 7.5, 7.9, 8.3 and 8.8, using PI, CS + PI and ROICS + PI methods on six channel data to compare proposed method with these conventional methods. The reconstruction error for the proposed method and the existing methods were quantified by Peak Signal to Noise Ratio (PSNR) using the formula

$$PSNR = 20log_{10}(\max(y)/\sqrt{sum(x-y)^2})/N \qquad (7)$$

where, x and y are ROICS-PI reconstructed and full k-space reconstructed image respectively and N is number of elements in x or y.

4 Results

ROICS on cardiac data: Figure 1(b) depicts a representative cardiac frame and the red outline depicts the chosen ROI. Difference between the conventional CS technique and novel ROICS can be observed in Figure 2. The noise in the reconstructed image using conventional CS increases with acceleration whereas ROICS technique is able to retain the details even at 10X. The resulting

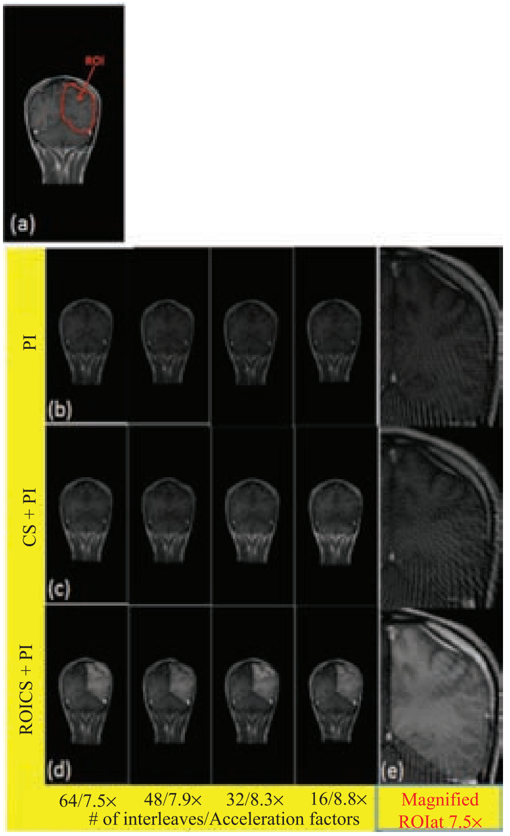

Figure 3: Reconstructed image: (a) ROI drawn on original/SoS image, (b) PI reconstruction, (c) CS + PI reconstruction, (d) ROICS + PI reconstruction, (e) ROI magnified image at 7.5x acceleration to compare proposed method with existing methods.

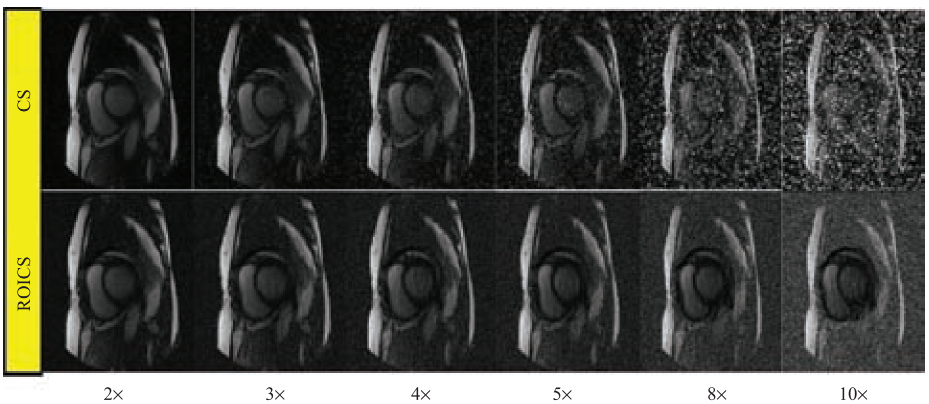

Figure 2: Comparison of conventional CS and proposed ROICS technique at different acceleration on cardiac data.

ROICS reconstruction with 10% of the data shown in Figure 2 (lower panel) demonstrates the utility of the proposed approach in an efficient manner. The graph in Figure 4 shows significant increase in the NRMSE value after 5x using conventional CS, whereas the increase in NRMSE value for ROICS is relatively insignificant.

ROICS-PI: The Sum of Squares (SoS) of the channels image with the ROI chosen for reconstruction is shown in Figure 3(a) for a representative data set. The results for the three methods over the 4 acceleration factors are shown in Figure 3(b): PI only; (c): CS + PI; and (d): ROICS + PI. It can be observed from these figures that ROICS + PI perform qualitatively better than the other two methods. Figure 3(e) depicts the magnified ROI at 7.5x depicting aliasing artefacts that can be observed in the other two methods arising due to the spiral trajectory, while ROICS+PI is able to reconstruct the image with significantly reduced aliasing artefacts. At acceleration values above 7.5x, it can also be observed that ROICS + PI has the least artefacts in the chosen ROI. The graph in Figure 5 shows the PSNR for ROICS and conventional reconstruction techniques for six data sets, and it can be noted that PSNR value for the ROICS method is higher compared to the other two techniques in case of each data for the specified ROI.

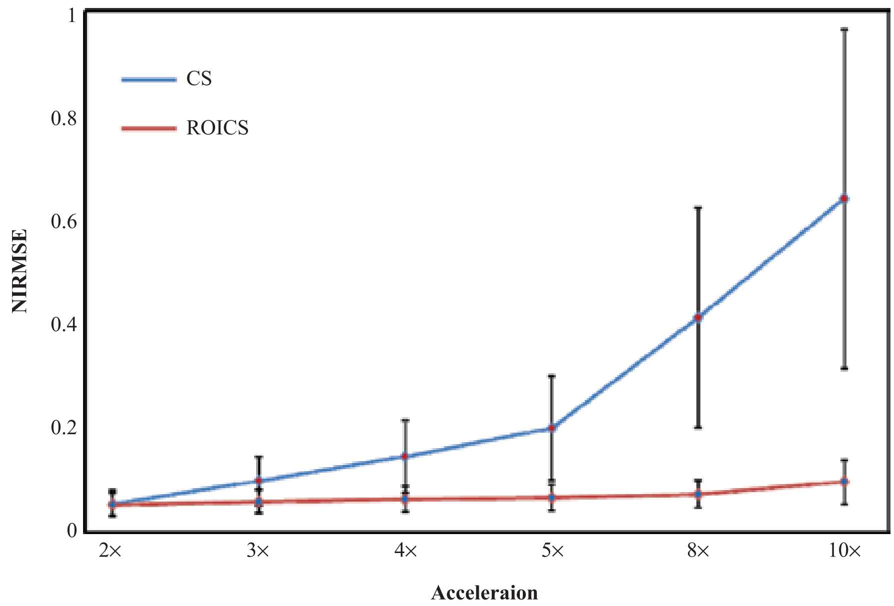

Figure 4: NRMSE comparison for cardiac data.

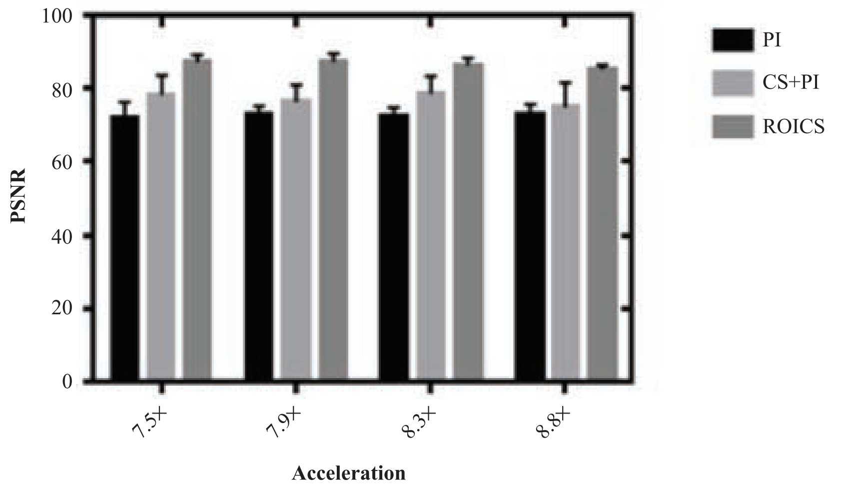

Figure 5: PSNR comparison (dataset 1 to data set 5) for 3 methods.

5 Discussion

ROICS performs better than conventional CS by limiting the reconstruction region, where surrounding or background regions are not important for further analyses. This sparse representation of data resulted in better reconstruction at higher acceleration factors compared to conventional CS. ROICS and conventional CS techniques were applied on cardiac and brain data, and as the acceleration increased, ROICS performed better in both the cases. ROICS on cardiac data was able to retain the details in the ROI selected region compared to CS, noticeably from 5x acceleration onwards. NRMSE value was calculated only in the ROI selected region for both ROICS and CS, as one is interested in the ROI region rather than the background, which is not required for further analysis. PI and CS are well-known methods used in MRI to reduce MRI acquisition time, and a combination of CS and PI was recently used to achieve better acceleration, instead of using PI or CS alone. Current method replaces the CS with ROICS to achieve better acceleration with PI. ROICS reconstruction technique has been applied by selecting common ROI on multiple channel data to make data sparse in each channel. It can be observed from Figure 3 that ROICS-PI performs better than PI alone or CS-PI. It can be observed that aliasing artifacts are present in the reconstructed images using PI alone and CS-PI due to highly undersampled spiral trajectories, while these artifacts are significantly reduced in the reconstructed image using ROICS-PI. An extension of ROICS could be performed either by using patch wise reconstruction by using a sliding window or patch wise reconstruction, although this would require a detailed understanding of the significant values in k-space for the relevant patches. Another important extension to the ROICS framework would be the optimizing of the k-space trajectories to acquire significant data by including it as part of the ROICS functional in Eq. [3]. ROICS technique can also be extended to other modalities such as CT and PET, where CS has been used.[24,25]

6 Conclusion

The development and application of ROICS has been performed here for the first time. ROICS allows for increasing the sparsity required for CS reconstructions by decreasing the number of non-zero coefficients to be estimated. It has been demonstrated qualitatively and quantitatively that ROICS outperforms CS at higher acceleration factors. ROICS technique was applied on cardiac and brain data to demonstrate its utility; ROICS on cardiac and brain data delivered better performance than the conventional CS and was quantified by evaluating the RMSE and PSNR respectively. A combination of ROICS and PI also has been demonstrated for the first time, and it was shown that it performs better than the other two methods such as PI alone and CS-PI qualitatively and quantitatively. The technique has been implemented for arbitrary k-space trajectories, and hence provides a general framework. Current and future work involves prospective application of ROICS through optimization of k-space trajectories for ROICS for diverse MR methods and integrating it with the reconstruction framework.

Acknowledgement

This work was supported by Vision Group of Science and Technology (VGST), Govt. of Karnataka, India under grant 'Technology Related Innovative Project' (TRIP) 2013–14, number 159718.

Received 10 June 2014.

References

1. Lustig, Michael, David Donoho, and John M. Pauly. Sparse MRI: The application of compressed sensing for rapid MR imaging. Magnetic resonance in medicine 58.6 (2007): 1182–1195.
2. Sairam Geethanath, Rashmi Reddy, Amaresha Shridhar Konar, Shaikh Imam, Rajagopalan Sundaresan, Ramesh Babu D.R, Ramesh Venkatesan. Compressed Sensing MRI: A review. Critical reviews in biomedical engineering 41.3 (2013): 183–204.
3. Larkman, David J., and Rita G. Nunes. Parallel magnetic resonance imaging. Physics in medicine and biology 52.7 (2007): R15.
4. Candès, Emmanuel J., Justin Romberg, and Terence Tao. Robust uncertainty principles: Exact signal reconstruction from highly incomplete frequency information. Information Theory, IEEE Transactions on 52.2 (2006): 489–509.
5. Jung Hong, Kyunghyun Sung, Krishna S Nayak, Eung Yeop Kim, and Jong Chul Ye. k-t FOCUSS: A general compressed sensing framework for high resolution dynamic MRI. Magnetic Resonance in Medicine 61, no. 1 (2009): 103–116.
6. Amaresha Shridhar Konar, Steen Moeller, Julianna Czum, Barjor Gimi, Sairam Geethanath. Region of interest compressive sensing (ROICS). In Proceedings of the 21st Annual Meeting of ISMRM, Salt Lake City, USA, 2013. p. 3801.
7. Kim, Yoon-Chul, Shrikanth S. Narayanan, and Krishna S Nayak. Accelerated 3D MRI of vocal tract shaping using compressed sensing and parallel imaging. IEEE, International Conference on Acoustics, Speech and Signal Processing (ICASSP) (2009) 389–392.

8. Murphy, Mark, Marcus Alley, James Demmel, Kurt Keutzer, Shreyas Vasanawala, and Michael Lustig. Fast 1-SPIRiT Compressed Sensing Parallel Imaging MRI: Scalable Parallel Implementation and Clinically Feasible Runtime. IEEE Transactions on Medical Imaging 31, no. 6 (2012): 1250–1262.
9. Liang D, Liu B, Wang JJ, and Ying L. Accelerating SENSE using compressed sensing. Magnetic Resonance in Medicine 62(2009): 1574–1584.
10. Wu B, Millane RP, Watts R, Bones P. Prior estimate-based compressed sensing in parallel MRI. Magnetic Resonance in Medicine 63(2011): 83 –95.
11. Fischer A, Seiberlich N, Blaimer M, Jakob P, Breuer F, and Griswold M. A combination of Nonconvex Compressed Sensing and GRAPPA (CS-GRAPPA). In proceedings of the 17th annual meeting of ISMRM, Hawaii (2009) P 2813.
12. Beatty PJ, King KF, Marinelli L, Hardy CJ, Lustig M. Sequential application of parallel imaging and compressed sensing. In proceedings of the 17th annual meeting of ISMRM, Hawaii (2009) P 2824.
13. Liu B, Sebert FM, ZouY, Ying L, SparseSENSE: Randomly-sampled parallel imaging using compressed sensing. In proceedings of the 16th annual meeting of ISMRM, Toronto, 2008, P 3154.
14. Zhao C, Lang T, Ji J. Compressed sensing parallel imaging. In proceedings of the 16th annual meeting of ISMRM, Toronto (2008) P 1478.
15. King KF. Combining compressed sensing and parallel imaging. In proceedings of the 16th annual meeting of ISMRM, Toronto, (2008) P 1488.
16. Amaresha Shridhar Konar, Divya Jain, Shamshia Tabassum, Rajagopalan Sundaresan, Ramesh Venkatesan, Sairam Geethanath. ROICS-PI: Combination of Region of Interest Compressed Sensing and Parallel Imaging for Arbitrary k-space Trajectories to Achieve Highly Accelerated MRI.In Proceedings of the 22nd Annual Meeting of ISMRM, Milan, Italy, 2014, P 1558.
17. Hansen, Per Christian, and Dianne Prost O'Leary. The use of the L-curve in the regularization of discrete ill-posed problems. SIAM Journal on Scientific Computing 14, no. 6 (1993): 1487–1503.
18. Grissom, William, Chun-yu Yip, Zhenghui Zhang, V Andrew Stenger, Jeffrey A Fessler, and Douglas C Noll. Spatial domain method for the design of RF pulses in multicoil parallel excitation. Magnetic resonance in medicine 56, no. 3 (2006): 620–629.
19. Pruessmann, Klaas P., Markus Weiger, Markus B. Scheidegger, and Peter Boesiger. SENSE: Sensitivity encoding for fast MRI. Magnetic resonance in medicine 42, no. 5 (1999): 952–962.
20. Griswold, Mark A, Peter M Jakob, Robin MHeidemann, Mathias Nittka, Vladimir Jellus, Jianmin Wang, Berthold Kiefer, and Axel Haase. Generalized autocalibrating partially parallel acquisitions (GRAPPA). Magnetic Resonance in Medicine 47, no. 6 (2002): 1202–1210.
21. Fessler, Jeffrey A, and Bradley P Sutton. Nonuniform fast Fourier transforms using min-max interpolation.IEEE Transactions on Signal Processing 51, no. 2(2003): 560–574.
22. Pruessmann, Klaas P., Markus Weiger, Peter Börnert, and Peter Boesiger. Advances in sensitivity encoding with arbitrary k-space trajectories. Magnetic Resonance in Medicine 46, no. 4 (2001): 638–651.
23. Dai, Yu-Hong, and Yaxiang Yuan. A nonlinear conjugate gradient method with a strong global convergence property. SIAM Journal on Optimization 10, no. 1 (1999): 177–182.
24. Chen, Guang-Hong, Jie Tang, and ShuaiLeng. Prior image constrained compressed sensing (PICCS): a method to accurately reconstruct dynamic CT images from highly undersampled projection data sets. Medical physics 35, no. 2 (2008): 660–663.
25. Choi, Kihwan, Jing Wang, Lei Zhu, Tae-Suk Suh, Stephen Boyd, and Lei Xing. Compressed sensing based cone-beam computed tomography reconstruction with a first-order method. Medical Physics 37, no. 9 (2010): 5113–5125.

Amaresha Shridhar Konar is currently working at Dayananda Sagar College of Engineering as an Assistant Professor at the Dept. of Computer Science and Engineering and as a Research Assistant in the Medical Imaging Research Center (MIRC). He has completed his M.Tech (2010) in Computer Networks Engineering from Visvesvaraya Technological University and is pursuing Ph.D at the Visvesvaraya Technological University. He has authored 8 peer reviewed publications and his research interests include developing novel technique for Magnetic Resonance Imaging (MRI) data acquisition and reconstruction.

Jain A. Divya is currently working as an Intern in MR coils team in GE Healthcare (March 2014–present). She is pursuing her M.Tech (2014) in Bio Medical Signal Processing and Instrumentation from Dayananda Sagar Institutions. Her research interests include development and application of novel techniques that helps in reducing the scan time in the domain of MRI.

Shamshia Tabassum is pursuing her M.Tech (2014) in Bio-Medical Signal Processing and Instrumentation from Dayananda Sagar College of Engineering, Bangalore. She has authored 4 peer reviewed publications and her research interests include development of novel acceleration techniques in MRI.

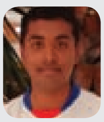

Rajagopalan Sundaresan is currently at General Electric as a Senior Design Engineer with a M.S. (2011) in Electrical and Computer Engineering from University of Arizona, USA. He has authored 5 conference publications and has one US patent. His research interests include development of new magnetic resonance methodologies for image reconstruction.

Julianna Czum is currently the director Cardiac Imaging and also Assistant Professor in Dept. of Radiology, Geisel School of Medicine, Dartmouth, United States. She has completed her MD (1993) from Robert Wood Johnson Medical School, Piscataway, NJ and She is Specialist in Cancer and Radiology.

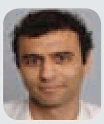

Barjor Gimi is currently director of the Biomedical NMR Research Center at Dartmouth and an Associate Professor of Radiology and of Medicine at the Geisel School of Medicine at Dartmouth. He received a dual-degree in physics (Lawrence University) and in mechanical engineering (Washington University in St. Louis). He worked in the biomedical industry before attending graduate school, receiving a doctorate in Bioengineering (University of Illinois at Chicago) and a postdoctoral degree in Radiology (Johns Hopkins University). His areas of research include cell engineering, nanofabrication methods for cell encapsulation, acquisition and reconstruction methods in MRI, and radio frequency microcoils for magnetic resonance microscopy.

Ramesh Babu D.R. is currently working at Dayananda Sagar College of Engineering as Professor and Head Dept. of Computer Science and Engineering. He has completed his M.Tech (1999) in Industrial Electronics and Ph.D (2004) from University of Mysore. He has authored more than 30 peer review publications. His research interests include developing image processing techniques for medical images and Unmanned Aerial Vehicles (UAV) tracking and navigation.

Ramesh Venkatesan joined Wipro GE Healthcare in late 1998 as an Advanced Applications Scientist in the MRI division where he is currently the Principal Engineer for Software and Applications Engineering at Wipro GE Healthcare. He has completed his M.S. (1993) in Biomedical Engineering from Case Western Reserve University, Cleveland and D.Sc. (1997) in Biological and Biomedical Engineering from Washington University in St Louis. He was then a senior research associate and Research Instructor at the Mallinckrodt Institute of Radiology, Washington University in St Louis (1997–1998). Author of 27 articles, several international conference abstracts and invited talks and co-author of a graduate-level textbook on Magnetic Resonance Imaging. Has 6 issued patents, 5 intellectual property publications, 1 trade-secret to his credit and has co-developed several innovations that are in different GE MRI products. His passion and research interests include development of clinically relevant MRI technologies that make MRI-based diagnostics easier to use and accessible to the currently unserved billions.

Sairam Geethanath is currently heading the department of Medical Electronics at Dayananda Sagar College of Engineering and is also directing the Medical Imaging Research Centre focussing on research related to magnetic resonance imaging. He graduated with a master's degree at the department of electrical engineering at Illinois Institute of Chicago, specializing in biomedical imaging and signals in 2007. He was also interning at Siemens Medical Solutions, Chicago, at the time working as a software developer in the department of Angiography and X-ray. He then went on to work as a full time software developer in the same department before pursuing his doctoral studies at the University of Texas Southwestern Medical Center at Dallas in 2008. His doctoral research focused on developing novel applications of compressed sensing to magnetic resonance imaging and spectroscopy, which he completed in 2011. Sairam pursued his post-doctoral fellowship for a year at the Imperial College of London in the Imaging Sciences Department working on parallel transmit MRI, before returning to his hometown: Bangalore. He has authored more than 27 peer reviewed publications.